Magnetic Properties of (VO)₂P₂O₇ from Frustrated Interchain Coupling

G. S. Uhrig¹ and B. Normand²

¹ Institut für Theoretische Physik, Universität zu Köln, D-50937 Köln
² Institut für Physik, Universität Basel, Klingelbergstrasse 82, CH-4056 Basel, Switzerland.
(December 2, 2024)

Neutron-scattering experiments on (VO)₂P₂O₇ reveal both a gapped magnon dispersion and an unexpected, low-lying second mode. The proximity and intensity of these modes suggest a frustrated coupling between the alternating spin chains. We deduce the minimal model containing such a frustration, and show that it gives an excellent account of the magnon dispersion, static susceptibility and electron spin resonance absorption. We consider two-magnon states which bind due to frustration, and demonstrate that these may provide a consistent explanation for the second mode.

PACS numbers: 75.10.Jm, 75.40.Cx, 75.40.Gb

Vanadyl pyrophosphate $((VO)_2P_2O_7)$, abbreviated $VOPO)^1$ is a low-dimensional quantum magnetic system composed of $S=\frac{1}{2}$ V^{4+} ions. These have Heisenberg antiferromagnetic (AF) interactions, and a singlet ground state¹ with spin gap $\Delta=3.1 \mathrm{meV}$. Based on susceptibility and neutron-scattering experiments on powders, VOPO has been compared in detail to spin-ladder and alternating-chain models,² both of which were found to be consistent with the data. Rising interest in spin ladders, along with the assumption that the strongest exchange paths would be those between V^{4+} ions with the smallest separations, led to a preference^{1,2} for the ladder conformation, and for several years VOPO was quoted as the first known spin ladder system.

This picture was conclusively debunked by Garrett and coworkers, who performed the first neutron-scattering measurements on aligned single crystals of VOPO.³ These demonstrated unequivocally that the strongest exchange path in the system (J_1) was a double V-O-P-O-V link through phosphate groups in the crystallographic bdirection, while the next (J_2) was a double V-O-V link between edge-sharing VO₅ square pyramids, also along \hat{b} . The V-O-V bond along \hat{a} through the apex of the pyramid, believed to be the strong ladder leg, was found to be very weak. The strength of the V-O-P-O-V bond was verified independently⁴ in the related compound $VODPO_4$. $\frac{1}{2}D_2O$, where it appears in isolation. These results are not unexpected, because the single electron on V^{4+} in a square pyramidal environment occupies the d_{xy} orbital in the basal (bc) plane of the unit. They lead to the interpretation of VOPO as a set of dimerized chains, with coupling ratio $\lambda = J_2/J_1 \simeq 0.8.^5$

The same experiment obtained the most detailed measurements to date for a second mode, first noted in a powder sample,⁶ which has a gap of 5.7meV and significant intensity over half of the Brillouin zone. This was identified from a previous study⁷ as a candidate two-magnon bound state. Furthermore, the coupling between the dimerized chains was deduced to be weakly ferromagnetic (FM), a result rather curious for a conventional, long superexchange path. We begin from the observation^{7,8} that frustration can act to promote bound states between ex-

citations, and the hypothesis that the FM interchain coupling in fact results from a competition between two AF couplings. We will deduce and justify the nature of such a frustrated, two-dimensional (2d) model for VOPO, and show that it provides the basis for a complete account of the magnetic properties of this material.

The structure of VOPO was determined in detail by Nguyen $et\ al.^9$ The b-axis alternating chains are coupled along \hat{a} by either the V-O-V path through apical O, or by V-O-P-O-P-O-V pathways through two PO₄ groups, while c-axis coupling (see also Ref. 1) proceeds through a single phosphate unit. Quantitative superexchange calculations, particularly for extended pathways, remain beyond the scope of current understanding and computer power, a particularly for the V ion. We adopt here a qualitative approach of identifying superexchange paths which couple strongly to the V d_{xy} orbital, and using consistency with experiment to construct the minimal set of necessary interactions.

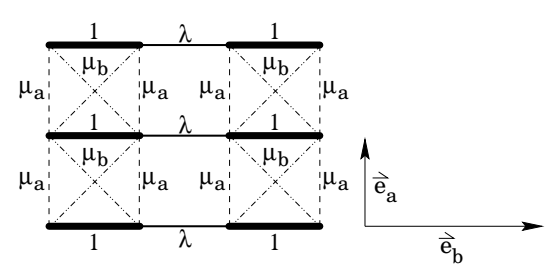


FIG. 1. Schematic representation of the VOPO system, showing frustrated coupling between dimerized chains.

We discard the possibility that the V-O-V bond along \hat{a} is significant, because its direction is orthogonal to the d_{xy} orbital. We argue instead in favor of the V-O-P-O-P-O-V path, due to the demonstrated importance of phosphate groups, and because bond angles throughout its length can remain close to 180° . Such paths connecting V ions separated only along \hat{a} (J_a), and those separated both along \hat{a} and by one ionic spacing along the chains (J_b), are in principle rather similar, which presents the possibility of frustration. However, there are 2 types of V-O-P-O-P-O-V path, those connecting into the phos-

phate groups mediating J_1 and those connecting to the O atom concerned in J_2 . If the latter were significant, one could expect in addition a strong c-axis coupling, which is not observed.³ We assume therefore that pathways of the second type are strongly suppressed by the angles and orbital configurations in the V-O-P overlap, and concentrate on the resulting 2d model in Fig. 1.

Here $J_1 = J$ is set to 1, λ is defined above, and $\mu_a = J_a/J$ and $\mu_b = J_b/J$ parameterize the competing V-O-P-O-P-O-V superexchange interactions. We exclude the possibility of a second-neighbor intrachain coupling, due to both the lack of a suitable exchange pathway and the minimacy criterion, as it is found not to be important to any of the quantities we will compute. That $\mu_{a,b}$ may be significant is shown immediately by considering 11 a high-temperature expansion of the static susceptibility $\chi(T)$. This yields the result that the Curie temperature θ_c should be given by the sum of the interactions of a structural unit according to

$$\theta_c = -\frac{1}{4}J[1 + \lambda + 2\mu_a + 2\mu_b]. \tag{1}$$

Comparison of the measured $\theta_c = -84 \text{K}^1$ with the values of the chain couplings³ suggests that the latter alone can satisfy at most 75% of the sum.

We analyze this model using the method of Ref. 11. Taking the strongest (J_1) bonds as the sites of dimers, whose singlet ground states may be excited to triplets, the interactions permit delocalization, or hopping, of the triplets. The hopping gives a kinetic energy which lowers the bond singlet-triplet gap to the physical one, and a description of a dispersive, triply-degenerate 1-magnon excitation in 2d reciprocal space. While this technique is best suited to strongly dimerized systems, perturbation-theoretic calculations¹¹ show rapid suppression of higher-order contributions even for rather weak dimerization, and thus internal consistency.

We have calculated the coefficients for hopping of a triplet excitation by perturbative expansion to 5th order in the parameters of Fig. 1, both along and between the chains. Contributions beyond 3rd order indeed remain small (3%), and we illustrate the method to this order. Let t_{ij} be the coefficient for the excited triplet to hop by i dimer bonds along the chain, and across j chains, and μ_{\pm} denote $\mu_a \pm \mu_b$, then

$$t_{00} = 1 - \lambda^{2}/16 + 3\lambda^{3}/64 + 3\mu_{+}^{2}/4 + 3\mu_{+}^{2}\mu_{-}/8$$

$$t_{10} = -\lambda/4 - \lambda^{2}/8 + \lambda^{3}/64 + \lambda\mu_{+}^{2}/16$$

$$t_{01} = \mu_{+}/2 - \mu_{+}^{3}/8 - 5\lambda^{2}\mu_{+}/32$$

$$t_{20} = -\lambda^{2}/16 - \lambda^{3}/64 \qquad t_{30} = -\lambda^{3}/128 \qquad (2)$$

$$t_{02} = -\mu_{+}^{2}/8 - \mu_{+}^{2}\mu_{-}/8 \qquad t_{03} = \mu_{+}^{3}/16$$

$$t_{11} = \lambda\mu_{+}^{2}/8 - \lambda^{2}\mu_{+}/32 + \lambda\mu_{+}\mu_{-}/16$$

$$t_{21} = 3\lambda^{2}\mu_{+}/64 \qquad t_{12} = -3\lambda\mu_{+}^{2}/32.$$

The mode dispersion is given most straightforwardly by

$$\omega(\mathbf{q}) = J \sum_{ij} 2^{(2-\delta_{i0}-\delta_{j0})} t_{ij} \cos(iq_y) \cos(jq_x), \qquad (3)$$

although in fact to this order one obtains a better fit by expanding the (smoother) quantity $\omega^2(\mathbf{q})$.

The measured dispersion data for the lowest-lying mode in Ref. 3, combined with the condition set by Eq. (1) from θ_c , allow one to deduce the model parameters providing the optimal fit. These are found to be the set

$$(J, \lambda, \mu_+, \mu_-) = (10.7 \text{meV}, 0.793, 0.203, 0.255),$$
 (4)

which correspond to the superexchange interactions

$$(J_1, J_2, J_a, J_b) = (10.7, 8.49, 2.17, 2.73) \text{meV}.$$
 (5)

The various fits offer minor differences in the exact shape of the dispersion curve, with the higher-order calculations returning a very good description of the overall form. For clarity we show only the 5th-order fits in Figs. 2 (a) and (b) for the reciprocal-space cuts where data is available. The results (4, 5) may be used to predict the form of the 1-magnon dispersion where it has not yet been measured, and this is shown in Figs. 2(c) and (d). We expect the upper band edge (at $(\pi/2, \pi/2)$ in the physical Brillouin zone) to be observed at 15.9meV.

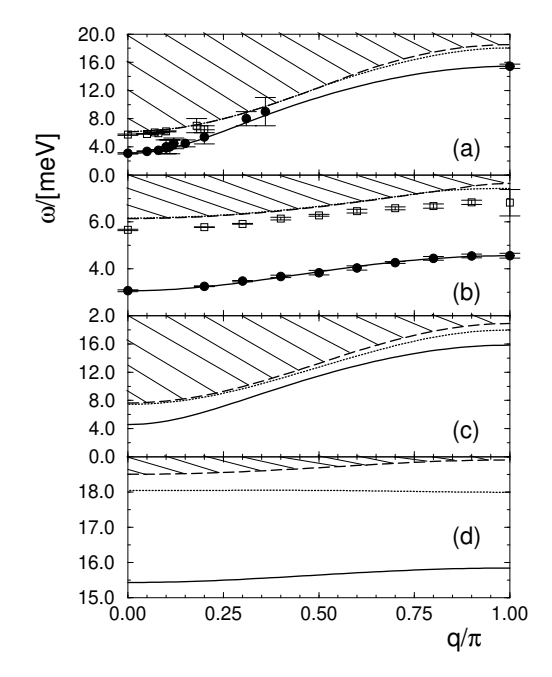


FIG. 2. Magnon dispersion (solid lines), continuum edge (dashed lines) and bound S=1 states (dotted lines) for (a) $(0.2\pi-q)$, (b) $(q.2\pi)$, (c) $(\pi,2\pi-q)$, and (d) $(2\pi-q,\pi)$. Symbols are data taken from Ref. [3].

The primary features of the optimal parameter set are as follows. The alternating chains have the rather weak dimerization $\lambda \simeq 0.8$, or $\delta = (1-\lambda)/(1+\lambda) \simeq 0.11$. The interchain couplings are significant, with a magnitude 20-25% of the primary chain energy scale. The cross coupling J_b is slightly larger than the pure a-axis coupling J_a , which is required for a net FM interchain dispersion, and fully plausible from the preceding considerations.

Fig. 3 shows the density of states determined from the dispersion. The dominant feature of this curve is the logarithmic singularity at the saddle point $(\pi/2,0)$, with energy 4.55meV. This energy, and not simply the the minimum gap $\Delta = 3.1$ meV at (0,0), will play a significant role in determining thermodynamic quantities.

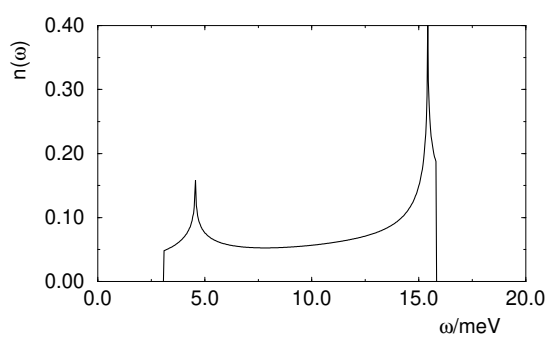


FIG. 3. Density of states for computed magnon dispersion.

We consider next the form of two further magnetic properties for which independent measurements are available, to determine the consistency of the model and parameters. The static, uniform susceptibility $\chi(T)$ was first measured for a powder sample by Johnston et al., 1 and quite recently for single crystals. 12 The susceptibility to applied field H measures available excitations with $\Delta S = 1$, so is primarily a probe of the 1-magnon branch. It is given in general by $\chi = -\partial^2 F/\partial H^2$, where $F = -\beta^{-1} \ln Z$ is the free energy and $\beta^{-1} = k_B T$. In the dimer model, an excited triplet is effectively a hard-core boson, because only one such state is physically possible on each bond. Thus the calculation of thermodynamic quantities requires a correction from Bose statistics to exclusion statistics appropriate for triply degenerate excitations. The free energy per dimer is 13

$$f = -\beta^{-1} \ln\{1 + [1 + 2\cosh(\beta h)]z(\beta)\},\tag{6}$$

where h denotes $g\mu_B H$ and $z(\beta)$ is the partition function for a single mode. The susceptibility per site is then

$$\chi_0 = \beta z(\beta) / \left(1 + 3z(\beta)\right),\tag{7}$$

in which the denominator suppresses the Bose result at high T by excluding multiple mode occupation.

While the statistical factor corrects for state availability, it does not take account of magnon interaction effects. These we may include within the following mean-field scheme. Approximating any Heisenberg interaction term with a spin on a neighboring dimer by $J_{i,i+\delta}\mathbf{S}_i\cdot\mathbf{S}_{i+\delta} \to J_\delta\langle S_i^z\rangle S_{i+\delta}^z \equiv J_\delta mS_\delta^z$, the instantaneous magnetization per site m contributes to an effective internal magnetic field

$$h_{int} = -mJ\lambda - 2mJ(\mu_a + \mu_b) \equiv -mC. \tag{8}$$

The susceptibility is defined by $m = \chi h_{ext}$, while the magnetization $m = \chi_0 h_{tot}$, where $h_{tot} = h_{ext} + h_{int}$ is the total field at each site. Simple rearrangement yields

$$\chi = \chi_0 / (1 + C\chi_0) \tag{9}$$

as the mean-field, interaction-corrected susceptibility, with $C = J(\lambda + 2\mu_+)$. For AF interactions this contributes only a suppression, and does not change the position of the maximum in χ_0 .

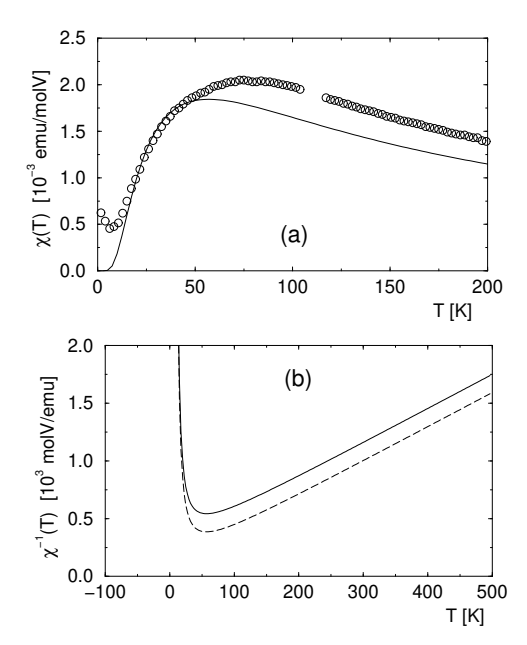


FIG. 4. (a) $\chi(T)$ from model parameter set. Deviations from measured data¹² are discussed in text. (b) $\chi^{-1}(T)$ with (solid line) and without (dashed) mean-field correction.

In Fig. 4(a) is shown the quantity $\chi(T)$ (9), with units converted to match experiment. The agreement with both powder and single-crystal data is good. Qualitatively, it is clear that both the exclusion statistics factor and (Fig. 4(b)) the mean-field correction are required to deduce $\chi(T)$ within this framework. Quantitatively, the temperature T_{max} of the peak susceptibility in the model is 58K, rather lower than both data sets, while the value χ_{max} is fractionally smaller. This latter result provides further evidence for the presence of frustrating interactions, whose mean-field correction provides the suppression appropriate to reproduce the data. From Fig. 4(b), the Curie temperature returned by the model treatment is in excellent agreement with the data.

The discrepancies between calculation and experiment may be analyzed by applying the triplet hopping theory with mean-field correction to the dimerized chain. For a chain with $\lambda=0.8$, the resulting $\chi(T)$ is directly comparable with essentially exact numerical simulations. ^{14,2} This comparison (with Figs. 2 of Refs. 14 and 2) reveals that $T_{max}^m/T_{max}^n \simeq 0.75$, while $\chi_{max}^m/\chi_{max}^n \simeq 1.2$, where superscripts m and n denote model and numerical results respectively. The former ratio is very similar to the discrepancy between model and experiment above. The latter suggests further that in 1d the mean-field correction is not sufficient to reproduce interaction-induced suppression of χ , whereas improved agreement is achieved in 2d.

We conclude that deviations from the data arise primarily because the calculational scheme cannot fully account for magnon interactions, and not due to any intrinsic shortcomings of the model.

ESR experiments have also been performed on powder and crystalline VOPO samples, and we focus here on the single-crystal results of Prokofiev $et~al.^{12}$ The strongest resonances are found at 134 and 288GHz, and enable the effective g-factor to be determined. The absorption at 134GHz shows 12 a thermally activated form which could be fitted with a single gap, but this alone did not yield a value consistent with neutron scattering results. For linearly-polarized (microwave) radiation, which excites transitions of $\Delta S^z = \pm 1$, the ESR power absorption is given 15 by the imaginary part of the susceptibility

$$\chi''(\omega) = \pi \delta(\hbar \omega - h) \sinh(\beta \hbar \omega) \int \frac{d^2 k}{(2\pi)^2} e^{-\beta \omega(\mathbf{k})}. \quad (10)$$

Including the hard-core boson constraint as above, the intensity at the resonance frequency $\hbar\omega = h$ is

$$I(\beta) \propto \frac{\sinh(\beta h)z(\beta)}{1 + (1 + 2\cosh(\beta h))z(\beta)}.$$
 (11)

This quantity contains in principle the mean-field correction in the form $h = h_{ext} - Cm$. However, for the resonance at 134GHz \sim 7K, the sinh function is linear at temperatures on the order of Δ , and alterations of h affect only the prefactor.

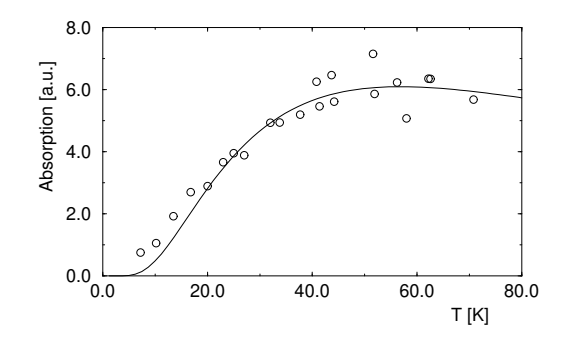


FIG. 5. ESR absorption from model parameter set, showing excellent consistency with observation. $^{\rm 12}$

The calculated ESR absorption is shown in Fig. 5 with the data of Ref. 12. The excellent agreement indicates the importance of the 2d density of states, in particular the energy scale of the logarithmic singularity (Fig. 3). While the ESR absorption is often considered to measure a q=0 property akin to $\chi(T)$, we note here a significant difference between the two in experiment. Theoretically, the triplet hopping approach yields a single energy scale for both quantities, which is in more satisfactory agreement with the ESR absorption, indicating that this is rather less sensitive than $\chi(T)$ to magnon interactions.

We conclude with a brief analysis of possible bound states of two magnons with the computed dispersion, to seek an explanation for the observed second mode. The initial perturbative problem, represented generally as $H = H_0 + \alpha H'$, may be brought by a continuous, unitary transformation 16 to a new Hamiltonian H_{eff} which conserves triplet number ($[H_{\text{eff}}, H_0] = 0$). This procedure is conducted perturbatively in α to generate a series for H_{eff} . The action of H_{eff} on the sector with one triplet gives the one-magnon dispersion, while on the two-triplet sector with total spin S = 1 it yields the two-magnon continuum and contains in addition magnon interactions. At fixed momentum one obtains a 2-body problem soluble by Lánczos tridiagonalization, in particular for the energy of (triplet) bound states. The number of interaction coefficients rises very rapidly with order n in α . We have completed calculations for n = 3 and 4, finding only small alterations ($\approx 2\%$ of the continuum edge energy), but caution that these remain potentially significant.

The predicted dispersion curves for the two-magnon bound state, computed at 4th order, are shown as the dotted lines in Fig. 2. We find that with the parameters fixed as above, the bound state does appear as an excitation mode below the continuum over a large part of the Brillouin zone. However, this is not the case close to the band minimum, where it is lost in the continuum. While we thus do not always find a second mode below 2Δ in a consistent treatment, the discrepancy between the computed bound state and the observed resonance is not large: it is reasonable to postulate that forthcoming refinement of this calculation, and possible extension of the model to include further interactions, will indeed yield a quantitative explanation of the second mode.

In summary, we have presented a model for frustrated, 2d coupling in $(VO)_2P_2O_7$. The model gives an excellent and fully consistent account of the available data concerning elementary excitations, namely the 1-magnon dispersion, static susceptibility and ESR absorption. We use it to predict the dispersion in the entire Brillouin zone, and to indicate the origin of the observed, low-lying second excitation mode as a triplet 2-magnon bound state.

During completion of this work, we became aware of the contribution of Weisse $et~al.^{17}$ These authors investigated the same model, albeit without the physical justification presented here, by diagonalization on small (up to 4×8) clusters. Their results are qualitatively in good agreement with our expectation that frustration should promote bound states. Quantitatively, the parameters chosen differ considerably, and we would not expect to see good agreement with susceptibility and ESR data.

We are grateful to U. Löw, B. Lüthi, S. Nagler, H. Schwenk, and particularly D. A. Tennant for invaluable discussions and provision of data. We thank also G. Bouzerar and E. Müller-Hartmann for helpful conversations, and C. Knetter for assistance with the calculation of $H_{\rm eff}$. GSU was supported by an individual grant and by SFB 341 of the DFG. BN wishes to acknowledge the generosity of the Treubelfonds.

- ¹ D. C. Johnston, J. W. Johnson, D. P. Goshorn, and A. J. Jacobson, Phys. Rev. B 35, 219 (1987).
- ² T. Barnes and J. Riera, Phys. Rev. B **50**, 6817 (1994).
- ³ A. W. Garrett, S. E. Nagler, D. A. Tennant, B. C. Sales, and T. Barnes, Phys. Rev. Lett. **79**, 745 (1997).
- ⁴ D. A. Tennant, S. E. Nagler, A. W. Garrett, T. Barnes, and C. C. Torardi, Phys. Rev. Lett. **78**, 4998 (1997).
- ⁵ T. Barnes, J. Riera, and D. A. Tennant, preprint # cond-mat 9801224, Phys. Rev. B (to appear).
- ⁶ A. W. Garrett, S. E. Nagler, T. Barnes, and B. C. Sales, Phys. Rev. B **55**, 3631 (1997).
- ⁷ G. S. Uhrig and H. J. Schulz, Phys. Rev. B **54**, R9624 (1996); Phys. Rev. B (to appear).
- 8 G. Bouzerar, A. P. Kampf, and G. Japaridze, preprint # cond-mat 9801046, Phys. Rev. B (to appear).
- ⁹ P. T. Nguyen, R. D. Hoffman and A. W. Sleight, Mat. Res. Bull. **30**, 1055 (1995).
- 10 M. Troyer and F. Mila, private communication.
- ¹¹ G. S. Uhrig, Phys. Rev. Lett **79**, 163 (1997).
- ¹² A. V. Prokofiev, F. Büllesfeld, W. Assmus, H. Schwenk, D. Wichert, U. Löw, and B. Lüthi, to be published.
- ¹³ M. Troyer, H. Tsunetsugu, and D. Würtz, Phys. Rev. B 50, 13515 (1994).
- ¹⁴ J. C. Bonner, H. W. J. Blöte, J. W. Bray, and I. S. Jacobs, J. Appl. Phys. **50**, 1810 (1979).
- ¹⁵ I. Affleck, Phys. Rev. B **46**, 9002 (1992).
- ¹⁶ F. J. Wegner, Ann. Physik **3**, 77 (1994).
- ¹⁷ A. Weisse, G. Bouzerar, and H. Fehske, preprint # condmat 9805374.